Received: 4 October 2023 | Revised: 18 May 2024 | Accepted: 20 May 2024

DOI: 10.1002/rcm.9842

RESEARCH ARTICLE

Rapid Communications in Mass Spectrometry WILEY

Isotopic and mineralogic bias introduced by pulverization of aragonite

Katharina E. Schmitt | Laura J. Fink | Anne Jantschke | Daniel Vigelius | Bernd R. Schöne

Institute of Geosciences, University of Mainz, Mainz, Germany

Correspondence
Katharina E. Schmitt and Bernd R. Schöne, Institute of Geosciences, University of Mainz, Johann-Joachim-Becher-Weg 21, 55128 Mainz, Germany.
Email: katharina.schmitt@uni-mainz.de and bernd.schoene@uni-mainz.de

Funding information
German Aerospace Center (DLR); German Federal Ministry of Education and Research (BMBF), Grant/Award Number: 01UL2001B; Deutsche Forschungsgemeinschaft; European Union's Horizon 2020, Grant/Award Number: 856488

Rationale: Stable carbon and oxygen isotope data of biogenic and abiogenic aragonite are of fundamental relevance in paleoclimate research. Wet-chemical analysis of such materials requires well-homogenized, fine-grained powder. In the present study, the effect of different grinding/milling methods on sample homogeneity and the potential risk of unintentional calcite formation and isotope shift were evaluated.

Methods: Shells of *Arctica islandica* and aragonite sputnik crystals were pulverized using a set of commonly used methods, including a hand-held drill, a vibromill operated at various settings (with and without liquid nitrogen cooling, changes in ball diameters, frequencies, and processing durations), and an agate mortar and pestle. Stable isotope values were measured using an isotope ratio mass spectrometer operated in continuous flow mode. Identification of mineral phases was obtained by powder X-ray diffraction (PXRD), Raman spectroscopy, and attenuated total reflectance-Fourier transform infrared (ATR-FTIR) spectroscopy. Calcite content was quantified by PXRD Rietveld refinement.

Results: Samples showed substantial homogeneity, in particular after vibromilling (duration 3–10 min). More vigorous grinding resulted in larger fractions of calcite (0.5–4.2 wt%) and a concomitant $\delta^{18}O$ and $\delta^{13}C$ decrease, specifically in bivalve shells. The only method for producing pure aragonite powder was by pounding the aragonite sputniks manually with an agate mortar and pestle.

Conclusions: None of the studied, commonly used machine-based pulverization methods produced pure aragonite powder from samples consisting originally of aragonite. These findings have significant implications for light-stable isotope-based paleoclimate reconstructions. Except for abiogenic aragonite powder produced by pounding in an agate mortar, paleotemperatures would be overestimated.

1 | INTRODUCTION

The $\delta^{13}C$ and $\delta^{18}O$ values of biogenic (e.g., bivalves, gastropods, corals) and abiogenic (e.g., speleothems) calcium carbonates are routinely used to reconstruct past climates and environments.[1–8] Depending on the material and the required level of spatial sampling resolution, various different techniques are employed to generate fine powder, which is required for wet-chemical analysis of the isotope composition. For detailed, high-precision sampling, computer-controlled[9–11] or manual micromilling or microdrilling using a drill affixed to a binocular microscope[12] or held in a hand[13] has been advised, whereas the pulverization and/or homogenization of

samples[14–18] can be accomplished by agate mortar pounding or ball milling,[19] which are the most efficient and straightforward methods to generate mineral powders.[20] However, to preserve the original mineralogical and isotopic properties of the carbonates, meticulous sample acquisition and preparation techniques are crucial.

In many experimental studies, different grinding, micromilling (or microdrilling), and pounding methods with varying settings were assessed to determine possible triggers, such as heat, pressure, or the amount of organic material, to understand the polymorphic transformation of aragonite into calcite and its effect on the isotopic composition.[21–29] However, none of these studies has focused on the homogeneity of the powder produced, nor have the methods been tested comparatively on both biogenic and abiogenic materials. Thus, the present study assessed the efficacy of the milling and pounding techniques commonly employed to produce carbonate powder and determined whether the temperature and pressure changes induced by different milling methods (and their configurations) affected the isotope signal of the pulverized sample. Furthermore, the study aimed to ascertain which method facilitated or impeded the conversion of aragonite into calcite with a view to improving the respective sample preparation techniques if necessary. Biogenic (shell of a live-collected bivalve mollusk from NE Iceland, *Arctica islandica*) and abiogenic (brown and white crystal sputniks) aragonite were pulverized using an agate mortar and pestle, a hand-held drill and (horizontal) vibrational mills. Vibromilling was accomplished with different settings (with and without liquid nitrogen as a coolant, combinations of different ball diameters, oscillation frequencies, and processing durations).

2 | EXPERIMENTAL

2.1 | Material

Shells of two *A. islandica* specimens (ICE12-08-A104; Arctica-1) collected alive in shallow waters of northeast Iceland and two aragonite sputnik crystals were selected from the paleontological collection of the Institutes of Geosciences, University of Mainz, Germany (Figure 1). Prior to the analysis, the periostracum was removed from both shells using a sandblaster (Figure 1A,B). To generate smaller sample fragments, both right valves as well as the brown and white aragonite sputnik crystals (Figure 1C,D) were first carefully crushed with a hammer. Individual shell fragments were sufficiently large and represented growth during multiple years, justifying the assumption that samples were isotopically largely identical prior to pulverization and individual fragments could be treated as aliquots of the same specimen.

2.2 | Assessment of original mineralogical composition: Raman spectrometry

Prior to pulverization, nine randomly selected spots on each arbitrarily selected sample fragment were analyzed using a Raman spectrometer to determine the original mineral composition. The measurements were carried out at room temperature using a Horiba Jobin Yvon LabRam spectrometer equipped with an Olympus BX41 optical microscope. A Nd:YAG laser (spot diameter ca. 5 × 5 µm) with a wavelength of 532.21 nm, a confocal hole of 400 µm, a grating with 1800 grooves/mm, an entrance slit width of 100 µm, and a 50× long-distance objective was employed. The LabSpec 6 Spectroscopy Suite software (Horiba Scientific) was used for material identification.

2.3 | Vibromilling, micromilling, and pounding

Sample fragments were used for three different pounding/milling methods with various settings (Figure 2): (i) manual pounding with an agate mortar and pestle for 5 min, (ii) vibrational ball milling in a CryoMill apparatus (Retsch GmbH, Germany) with liquid nitrogen as cooling agent (hereafter referred to as "cryomill" or "cryogenic

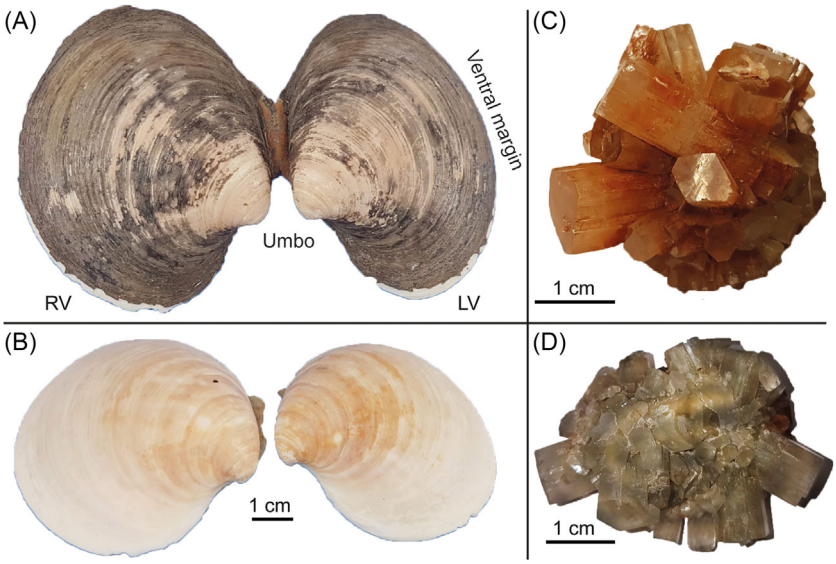

FIGURE 1 Right (RV) and left (LV) valves of an aragonitic bivalve shell, *Arctica islandica* (ICE12-08-A104) with (A) and without (B) periostracum (protective organic layer on the outer shell surface) with indicated umbonal region and ventral margin. (C) Brownish/reddish (Unikat no. 17) and (D) white (Unikat no. 06) aragonite sputniks. [Color figure can be viewed at wileyonlinelibrary.com]

vibromill" method), and (iii) the same settings and same machine as above, but without any cooling agent (hereafter referred to as the "vibromill" method). Grinding settings included combinations of differently sized stainless-steel milling balls (Ø 10 and 15 mm), different processing durations (3, 5, and 10 min), and different oscillation frequencies (10, 20, and 25 Hz). Note that only one stainless-steel milling ball was used in each vessel for these vibromilling methods. (iv) To evaluate the potential for further improved sample homogeneity and assess the isotopic and mineralogic effects of a second grinding cycle, Arctica-1 underwent two different vibromilling cycles. Shell fragments were first processed in a vibromill (Retsch Mixer mill MM200) equipped with zirconium oxide jars and two ZrO_2 milling balls (Ø: 10 mm) (Figure 2: "1st," sample hereafter referred to as "$Arctica_{MM}$"). Subsequently, the $Arctica_{MM}$ powder was further homogenized using the cryomill operated with one stainless-steel milling ball (Ø: 15 mm; oscillation frequency: 25 Hz, time: 5 min) (Figure 2: "2nd," hereafter "$Arctica_{CM}$"). (v) Furthermore, shell powder representing multiple years of growth was obtained from the left valve of *A. islandica* specimen ICE12-08-A104 using a Rexim Minimo hand-held drill equipped with galvanically bound diamond drill heads (for details see Data S1) operated at 2000 rotations per minute.

2.4 | Stable isotope analysis

Prior to the isotope analysis, all samples were dried for 24 h in an oven at 30°C. Ten to fifteen aliquots (50–120 µg) of each pulverized sample were dissolved in water-free phosphoric acid at 72°C in He-flushed 12-mL borosilicate exetainers. Generated CO_2 was measured with a Thermo Fisher Scientific MAT 253 continuous flow isotope ratio mass spectrometer coupled to a GasBench II. Isotope data were calibrated against a Carrara marble standard (distributed by IVA Analysentechnik GmbH & Co. KG, Meerbusch, Germany) and NBS-18 (two-point calibration). The $\delta^{18}O$ values were not corrected for differences in the acid fractionation factor (AFF) of aragonite and calcite.[30] The homogeneity of each $CaCO_3$ powder was assessed from the 1σ standard deviation of the mean of the 10 measured sample aliquots and the propagated error of the average analytical uncertainty ($\delta^{13}C$: 0.03‰ and $\delta^{18}O$: 0.06‰).

2.5 | Mineralogical analysis

X-ray diffraction (XRD) data were acquired using a Seifert XRD 3000 TT diffractometer. The instrument was equipped with a secondary graphite monochromator and operated with Cu-Kα1 radiation (40 kV, 30 mA). Powder samples underwent scanning in the 2Θ range of 20–40°, with a counter time of 2 s per step and a step width of 0.03°. RayfleX Analyze software (ver. 2.370) was employed to deconvolve the diffractograms and a quantitative determination of the calcite content was achieved by Rietveld refinement using the Profex software (ver. 5.2.7).[31] Since the abiogenic materials contained other mineral phases, for example periclase, the calcite-to-aragonite ratio was scaled to 100%. Typical detection and quantification limits (for Cu patterns) were 0.2 and 0.1 wt%, respectively, with an uncertainty of ca. 100%. Lower uncertainties (e.g., 20%) require larger amounts (e.g., 1 wt%).[32]

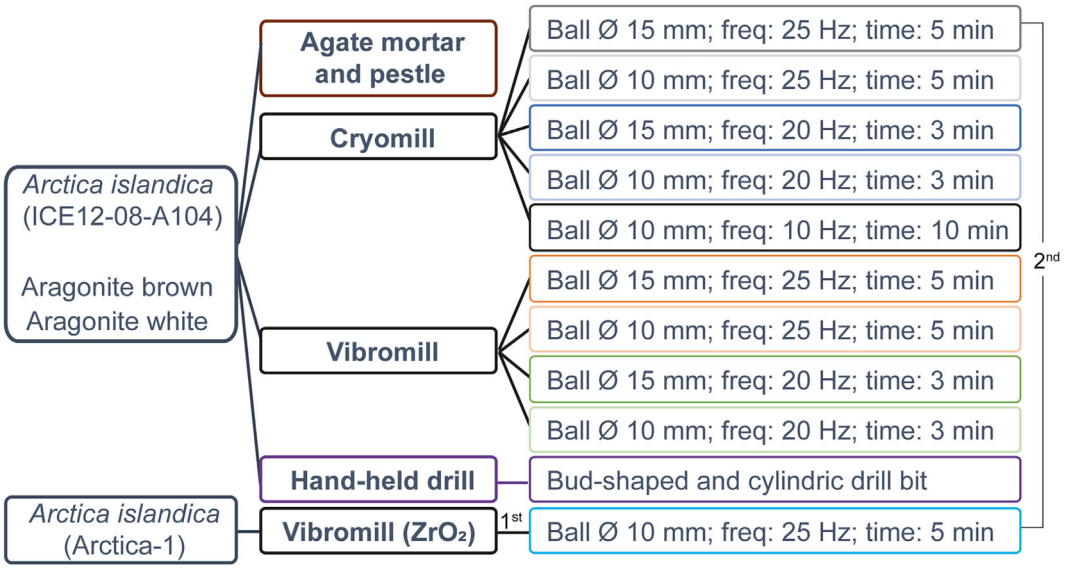

FIGURE 2 Scheme of the processing methods applied to a *Arctica islandica* shell (ICE12-08-A104) and to two aragonite sputniks, using different pounding and griding/milling methods, that is, combinations of differently sized stainless-steel milling balls (Ø 10 and 15 mm), different processing durations (3, 5, and 10 min), and different oscillation frequencies (freq; 10, 20, and 25 Hz) as well as the use of liquid nitrogen as cooling agent (cryomill) and without N_2 (vibromill). The valve of Arctica-1 was milled twice. The first powder was generated using a vibromill equipped with ZrO_2 milling balls and jars (1^{st}), and the second grinding was conducted by cryomilling using a single stainless-steel ball and jar (2^{nd}). [Color figure can be viewed at wileyonlinelibrary.com]

All materials were subjected to attenuated total reflectance–Fourier transform infrared (ATR-FTIR) spectroscopy using a Thermo Scientific Nicolet 6700 FTIR with a DTGS KBr detector equipped with an attenuated total reflectance crystal accessory (ATR Golden Gate). FTIR spectra were recorded between 4000 and 420 cm^{-1} using 100 scans and a spectral resolution of 2 cm^{-1}. The data were subjected to analysis using OMNIC™ software.

3 | RESULTS

3.1 | Sample homogeneity

All tested methods produced well-homogenized powders as evidenced by a low spread (1σ) of the mean $\delta^{13}C$ (range 0.03‰–0.10‰, average 0.05 ± 0.01‰) and $\delta^{18}O$ data (range 0.07‰–0.12‰, average 0.08 ± 0.01‰) of the 10 measured aliquots of each sample (Table 1). With 0.08 ± 0.02‰ ($\delta^{13}C$) and 0.09 ± 0.01‰ ($\delta^{18}O$), the mortar and Apestle method yielded, overall, the least homogeneous results (Table 1). A second milling cycle with the cryomill further increased the sample homogeneity of the shell powder (1σ $\delta^{18}O$: from 0.12‰ to 0.09‰; 1σ $\delta^{13}C$: from 0.06‰ to 0.04‰; Figure 3D), but also led to significant differences in the $\delta^{18}O$ values (one-way ANOVA; $p = 0.967$).

3.2 | Pulverization caused partial formation of calcite and negative isotope shift

Raman spectroscopy of the fragments revealed that all the studied materials were pure aragonite prior to pulverization (Data S1). After pulverization, however, only the abiogenic aragonite powder produced with an agate mortar and pestle was still pure aragonite (XRD analysis including Rietveld refinement 0 wt% calcite; Table 1). All other pulverization methods resulted in the partial formation of calcite, with the shell powders containing larger amounts of calcite (1.3–4.2 wt%) than abiogenic $CaCO_3$ powders (brown aragonite 0.5–2.7 wt%, white aragonite 0.7–2.5 wt%) (Table 1). Shell powder produced with the agate mortar and pestle revealed the presence of 0.8 wt% calcite. Shell samples ground with a large ball (Ø: 15 mm) contained between 0.5 and 1.7 wt% more calcite than powder generated with a smaller ball diameter (Table 1 and Figure 3A). Regrinding of $Arctica_{MM}$ powder in the cryomill led to a distinct increase in the calcite content from 1.49 to 7.34 wt% (Table 1).

Stable oxygen and carbon isotope ($\delta^{18}O$, $\delta^{13}C$) values of abiogenic and biogenic powders produced with agate mortar and pestle were higher than those generated with any studied machine-based grinding/milling method (hand-held drill, vibromill or cryomill) (Figure 3 and Table 1). The $\delta^{18}O$ values of shell powder decreased gradually (non-linearly) as calcite content increased. The strongest $\delta^{18}O$ offset (-0.63‰) and highest calcite content (4.24 wt%) were observed after the most vigorous grinding without liquid nitrogen (ball Ø 15 mm, freq. 25 Hz, duration 5 min; Figure 3A). For $\delta^{13}C$, the trend was less distinct (and statistically insignificant), but likewise negative (strongest shift of -0.93‰ with the same method as above). In the abiogenic materials, no clear-cut relationship was observed between calcite content, kinetic energy, and $\delta^{18}O$ values, but a weak negative correlation was observed in the case of $\delta^{13}C$, statistically significant for the white aragonite sputnik (Figure 3B,C). In general, much less calcite formed during grinding/milling of abiogenic aragonite and isotope shifts were less severe than in biogenic aragonite. Oxygen isotopes were shifted by up to -0.43‰ and -0.24‰ for powders generated from the white and brown sputniks, respectively, and their $\delta^{13}C$ values were ca. 0.3‰ lower than powder generated in the agate mortar (Figure 3B,C).

In case of shells, the use of a larger milling ball led to an increase in calcite content, but did typically not result in a noticeable $\delta^{18}O$ shift, unless the most vigorous grinding method without liquid nitrogen was applied (Figure 3A). However, there was a tendency for lower $\delta^{13}C$ values in conjunction with increased amounts of calcite when shell material was ground with a larger milling ball (Figure 3A). Except for the least vigorous cryomilling (ball Ø 10 mm, freq. 20 Hz, duration 3 min), abiogenic aragonite powders likewise contained increasingly more calcite and ^{12}C when grinding was completed with a larger milling ball (Figure 3B,C). With few exceptions, for the same combination of ball size, oscillation frequency, and duration of treatment, larger fractions of calcite were produced when shell material was ground with liquid nitrogen, but without a noteworthy effect on isotopes (Figure 3). This finding was corroborated by cryomilling of pre-existing shell powder ($Arctica_{MM}$) that resulted in unchanged $\delta^{13}C$ and only negligibly (ca. 0.1‰) lower $\delta^{18}O$ values, despite a massive increase in the proportion of calcite (Figure 3D).

Hand-held micromilling generated similar amounts of calcite and resulted in similar isotope shifts as the most vigorous vibromilling (Figure 3).

4 | DISCUSSION

As demonstrated here, it was impossible with any of the tested machine-based pulverization methods (micromilling, vibromilling, and cryomilling) to produce pure aragonite powder from biogenic (bivalve shell) or abiogenic (monocrystalline) aragonite. Only the powder produced from the aragonite sputniks with the agate mortar and pestle by hand remained mineralogically unchanged. One may question if the shell originally consisted entirely of aragonite and argue that patches of calcite may have existed below surface, that is, at locations which were missed by Raman spectroscopy. However, none of the arbitrarily chosen spots in the shell fragments measured by means of Raman spectroscopy revealed any traces of calcite. Calcite was also not reported previously in shells of *A. islandica*,[33–37] including Holocene fossils,[38] and was not detected in specimens treated with Feigl solution[38,39] (B.R. Schöne, unpublished data) or fragments assessed with FTIR spectroscopy (Data S1).

TABLE 1 Summary of the mean (Ø) and standard deviation (1σ) (including propagation of analytical uncertainty) of the stable oxygen and carbon isotope values and the calcite content (wt%) calculated by Rietveld refinement for the various settings, including different milling ball diameters (ball Ø), frequencies (freq.), and processing durations (time).

		Material					
		Artica islandica shell (Arctica-1)			Artica islandica shell (ICE12-08-A104)		
Method		Ø ± 1 σ $\delta^{18}O$ (‰)	Ø ± 1 σ $\delta^{13}C$ (‰)	Calcite (wt%)	Ø ± 1 σ $\delta^{18}O$ (‰)	Ø ± 1 σ $\delta^{13}C$ (‰)	Calcite (wt%)
	Vibromill (ZrO_2)	2.48 ± 0.12	1.92 ± 0.06	1.49			
	Hand-held drill				2.70 ± 0.07	1.88 ± 0.05	3.83
	Agate mortar				3.10 ± 0.10	2.22 ± 0.10	0.84
Cryomill	Ball Ø: 15 mm Freq.: 2 Time: 5 min	2.35 ± 0.09	1.92 ± 0.04	7.34	2.95 ± 0.09	1.60 ± 0.04	3.31
	Ball Ø: 10 mm Freq.: 25 Hz Time: 5 min				2.89 ± 0.07	2.14 ± 0.05	2.77
	Ball Ø: 15 mm Freq.: 20 Hz Time: 3 min				2.94 ± 0.08	1.31 ± 0.06	2.81
	Ball Ø:10 mm Freq.: 20 Hz Time: 3 min				3.02 ± 0.07	1.81 ± 0.05	2.27
Vibromill	Ball Ø: 15 mm Freq.: 25 Hz Time: 5 min				2.47 ± 0.10	1.56 ± 0.08	4.24
	Ball Ø: 10 mm Freq.: 25 Hz Time: 5 min				2.90 ± 0.09	1.83 ± 0.06	2.59
	Ball Ø: 15 mm Freq.: 20 Hz Time: 3 min				3.01 ± 0.10	1.29 ± 0.06	1.8
	Ball Ø: 10 mm Freq.: 20 Hz Time: 3 min				3.01 ± 0.07	2.09 ± 0.04	1.32

TABLE 1 (Continued)

Method	Material						Number of aliquots
	Aragonite white			Aragonite brown			
	Ø ± 1 σ $\delta^{18}O$ (‰)	Ø ± 1 σ $\delta^{13}C$ (‰)	Calcite (wt%)	Ø ± 1 σ $\delta^{18}O$ (‰)	Ø ± 1 σ $\delta^{13}C$ (‰)	Calcite (wt%)	
							15
	−7.22 ± 0.07	7.02 ± 0.05	2.31	−7.17 ± 0.12	7.18 ± 0.06	1.85	10
	−6.90 ± 0.09	7.34 ± 0.07	0.00	−6.94 ± 0.08	7.46 ± 0.06	0.00	10
Cryomill	−7.20 ± 0.08	7.21 ± 0.04	2.53	−7.16 ± 0.09	7.23 ± 0.04	2.27	Artica-1:15
							10
	−7.14 ± 0.08	7.24 ± 0.04	1.51	−7.15 ± 0.07	7.30 ± 0.04	1.23	10
	−7.26 ± 0.07	7.27 ± 0.04	0.66	−7.11 ± 0.08	7.40 ± 0.04	1.53	10
	−7.15 ± 0.10	7.31 ± 0.05	1.10	−7.17 ± 0.09	7.26 ± 0.05	0.46	10
Vibromill	−7.03 ± 0.09	7.10 ± 0.03	2.09	−7.13 ± 0.07	7.18 ± 0.04	2.70	10
	−7.08 ± 0.07	7.24 ± 0.04	1.80	−7.08 ± 0.07	7.35 ± 0.04	2.54	10
	−7.32 ± 0.07	7.18 ± 0.04	1.62	−7.17 ± 0.08	7.38 ± 0.06	1.26	10
	−7.16 ± 0.07	7.32 ± 0.04	1.41	−7.12 ± 0.08	7.41 ± 0.04	0.92	10

4.1 | Machine-grinding/milling of aragonite: implication for paleoclimate reconstructions

The fractional inversion of aragonite to calcite during machine-based pulverization has implications for paleoclimate reconstructions, first because it was associated with a negative $\delta^{18}O$ and $\delta^{13}C$ shift (Figure 3). For example, per 1 wt% increase of calcite, $\delta^{18}O$ values of the shell powder dropped, on average, by 0.15‰ ($p < 0.01$; Figure 3). As discussed further below, however, the isotope change may not be solely linked to the formation of calcite, which could explain why the relationship between isotope value and calcite content was not always statistically significant. Secondly, the fraction of calcite in the aragonite powder needs to be considered when $\delta^{18}O$ values are computed[28] because the AFF differs for both $CaCO_3$ polymorphs.[40]

Even if the $\delta^{18}O$ value was properly corrected for differences in AFF (which would not be possible for the shell because hand-pounding did not produce pure aragonite powder), it would reflect the temperatures during formation of both aragonite and calcite. Isolating the aragonite precipitation temperature would require knowledge of the isotope composition of the fluid (or water vapor and/or atmospheric CO_2) and temperature that were present when calcite formed. This information, however, is missing. It should be added that many aragonites – including those used in the present paper (see Data S1) – also contain amorphous calcium carbonate (ACC), which likewise comes with an AFF that deviates from such of aragonite and calcite. Furthermore, decomposition of shell organic matrix at temperatures between ca. 80 and 175°C (the temperature at which calcite starts to precipitate under wet conditions) can induce the precipitation of abiogenic aragonite.[37] Its relative amount and environmental conditions during formation would likewise need to be considered in paleotemperature reconstructions. Given these challenges, we refrained from providing AFF-corrected $\delta^{18}O$ values.

In the case of the *Arctica* shell, even manual grinding with an agate mortar and pestle resulted in aragonite powder with 0.8 ± 0.3 wt% (average ± 1σ) calcite. This finding was surprising as it is commonly assumed that powder produced from aragonitic biominerals by hand-grinding remains mineralogically unchanged and does not undergo enantiotropic transformation (e.g., Waite & Swart[26]). The possible reasons for this will be discussed further below. Considering the slope of the regression line ($\delta^{18}O$ shift vs. calcite content), the $\delta^{18}O$ value of the original *Arctica* shell may have been ca. 0.1‰–0.2‰ higher than the powder generated with the agate mortar and pestle. Future studies should test if other biominerals consisting of pure aragonite likewise show fractions of calcite after pulverization by hand in an agate mortar and assess potential taxon-specific differences.

Irrespective of material (biogenic or abiogenic), slightly more homogenous aragonite powder than that generated by manual grinding was obtained by micromilling and vibromilling, but on the expense of larger calcite fractions and lower isotope values (Table 1 and Figure 3A–C). To place the observed oxygen isotope data in paleoclimatological context: If the occurance of the fractional calcite in the sample remained unnoticed, the $\delta^{18}O$ shift of -0.3‰ (aragonite

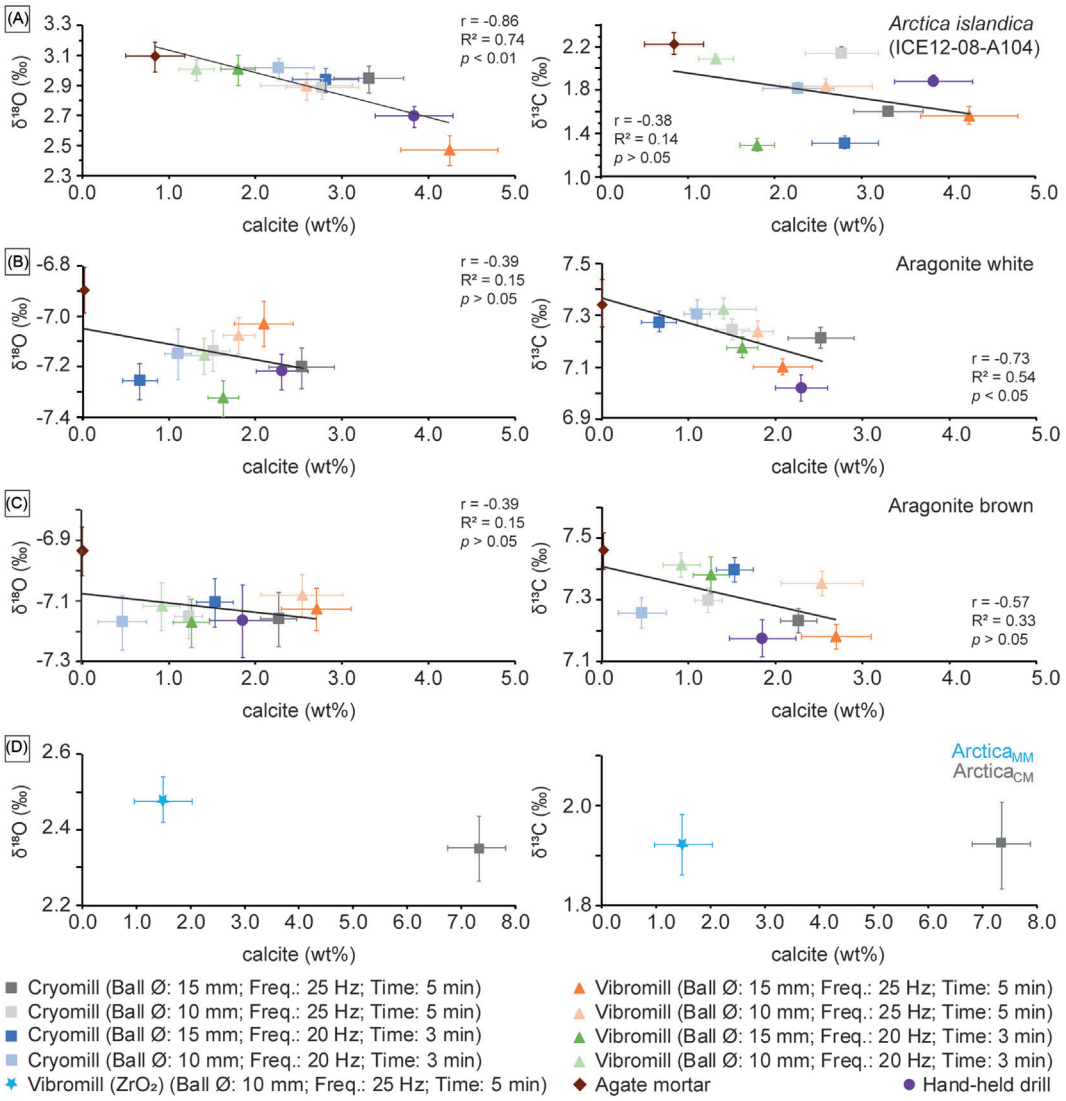

FIGURE 3 Isotope-ratio mass spectrometry and X-ray diffraction data of biogenic (*Arctica islandica* shells, right valves; A = ICE12-08-A104, D = Arctica-1) and abiogenic $CaCO_3$ powders (B: white aragonite sputnik; C = brown aragonite sputnik). Error bars indicate 1σ of the calcite content resulting from the Rietveld refinement, and in case of the isotope data, error bars indicate 1σ of the mean of the 10 aliquots with propagated error (i.e., including 1σ analytical uncertainty). [Color figure can be viewed at wileyonlinelibrary.com]

sputniks) to -0.4‰ (shell) by micromilling (at 2000 rpm) relative to the agate mortar and pestle powder (Table 1) would result in an overestimation of actual temperatures by ca. 1.3 to 1.7°C, respectively. The strongest observed oxygen isotope shift of -0.63‰ (shell) caused by forceful vibromilling would translate into 2.7°C higher than actual water temperatures during mineralization if the fractional calcite formation remained unnoticed and the paleothermometry equation for aragonite was used.

4.2 | Mineralogical and isotopic change: stress-induced polymorphic transformation

The observed isotopic shifts most likely resulted from a combination of causes that differed for manually pound, micromilled, and (non/cryogenically) vibromilled aragonite powders. If the specific set of causes is known, recommendations can be provided to reduce isotope biases and limit the fractionate formation of calcite or other secondary precipitates.

The drop in isotope values and increase in neomorphic calcite content of vibromilled samples can best be explained by the **mechanochemical inversion of aragonite to calcite**.[22,41] Vibrational ball milling accelerates solid-state diffusion rates (which otherwise occur on geological time-scales), facilitating the polymorphic transformation of minerals as well as isotopic exchange reactions with the ambient environment.[42] Reaction kinetics increased with higher oscillation frequency, larger balls, and longer grinding duration (cf. Schmidt et al.[43]) and resulted in larger amounts of fractional calcite and lower isotope values (Table 1 and Figure 3). Thus, the mechanical stress increased the surface area and number

of lattice distortions and thus generated more calcite nucleation sites.[41]

The stronger decline of isotope values in shell powders compared to abiogenic aragonites vibromilled at the same settings could be explained by the presence of an organic matrix that provided an extra source of oxygen and carbon for isotope exchange.[28] Further support for this assumption comes from the fact that more energetic milling regularly resulted in lower $\delta^{13}C$ values. An additional thermal decomposition of the organic matrix during vibromilling would have resulted in voids[37] that facilitated the structural reorganization associated with calcite formation[44] considering the 8 vol% increase during transformation.[45] Furthermore, a larger calcite fraction in shell powder could root in a different ultrastructure and lower crystallinity than in abiogenic aragonite as well as anisotropic lattice distortions[46–48] that facilitated calcite formation.

The absence of calcite in hand-grown aragonite sputniks may be explained by lower kinetic energy and less complex stress conditions than those generated by vibrational ballmilling. While vibromilling fosters the mechanochemical inversion of aragonite into calcite,[49] manual pounding with a mortar and pestle does not[41] because it typically does not induce slip planes along aragonite (001),[41] which are required for transformation to calcite.[50] However, the fractional formation of calcite, potentially resulting from the transformation of ACC, in the aragonitic shell powder produced by manual pounding was surprising. It is hypothesized here that the presence of proteinaceous sheets along aragonite (001) planes (cf. Nassif et al.[51]) facilitated the generation of respective slip planes when ground with a mortar and pestle. Although organic material was also detected in the studied abiogenic aragonites (Data S1), it likely occurred along cracks and lattice distortions rather than along aragonite (001) ("the most closely packed plane"[41]). Future studies should determine the composition of this organic material in the aragonite sputniks and assess its origin.

4.3 | Mineralogical and isotopic change: low-temperature effects

Temperature generated during vibrational ball milling can further increase reaction kinetics. However, neither the grinding stock[43] nor the cores of individual particles[22] heat up sufficiently to initiate a (dry) thermal inversion of aragonite to calcite,[42] which would require temperatures of around 400°C.[52] In our experiments, the temperature of the grinding stock remained below 33°C, which is line with previous observations.[43] However, we cannot preclude that somewhat higher temperatures were locally attained at the surface of (bio)mineral grains during collision with the milling balls. Should temperatures at the impact spots of the aragonite particles have exceeded 80°C, organic matrices may have decomposed and – provided that sufficient volatiles (H_2O, CO_2) were available as reaction partners, for example, liberated from decaying organic material – **abiogenic aragonite** may have precipitated (cf. Forjanes et al.[37]). This would be associated with a stronger decrease in $\delta^{18}O$ and $\delta^{13}C$ values than expected for a given calcite fraction (i.e., assuming a linear relationship between isotope values and calcite content when less forceful ground) or an isotope decline without change in calcite content (as observed, e.g., by Staudigel & Swart[27] and Moon et al.[29]). However, our data do not verify this assumption. While the most vigorous vibromilling of shell aragonite led indeed to a stronger $\delta^{18}O$ shift than expected for the estimated calcite content, corresponding stable carbon isotope values showed no unusual decline (note that the relationship between $\delta^{13}C$ and calcite content was statistically insignificant). Furthermore, the additional use of nitrogen as a coolant should have reduced the formation of abiogenic aragonite and resulted in higher isotope values, which likewise is only the case for $\delta^{18}O$ but not $\delta^{13}C$ (Table 1 and Figure 3).

4.4 | Mineralogical and isotopic change: temperature-induced polymorphic transformation

In contrast to vibrational ball milling, micromilling typically generates much more heat, specifically when operated at higher speed and with stronger contact pressure[29]. Such conditions enable the **thermal inversion of aragonite to calcite** (here likely in addition to mechanochemical transformation), which include dissolution (of aragonite) and recrystallization (as calcite)[24] and – as long as exchange partners have a lower isotope signature than the original aragonite – decreased $\delta^{18}O$ and $\delta^{13}C$ values.[26,27,29,53–55] As in the case of mechanochemical transformation, stronger isotope shifts and higher calcite contents in shell powder can be explained by the presence of an organic matrix that catalyzes and/or facilitates polymorphic transformation and isotopic exchange reactions. Temperatures at the immediate contact zone between the rotating drill bit and the sample can hardly be directly measured, but if thermal inversion was at play the required temperatures can be derived from experiments in which abiogenic and biogenic aragonite powders were gradually heated.

Under dry conditions, the conversion of abiogenic aragonite to calcite starts between 385°C[25] and 400°C[52] and takes several hours to complete. At higher temperatures (470°C), no aragonite is left after a several minutes (e.g., Epstein & Mayeda[56]). Trace impurities increase the inversion temperature.[52] The thermal decomposition of $CaCO_3$ starts at around 600°C.[28] In the absence of external water, biogenic aragonite starts to convert to calcite earlier than abiogenic aragonite, that is, at around 300°C.[27,57,58] Other authors reported higher temperatures of ca. 375°C.[25,59] The fairly abrupt increase in calcite formation around 400°C is linked to the decay of the intra-crystalline organic matrix[28] leading to an increase in porosity[60] and larger reaction surfaces. Under hydrothermal conditions (wet thermal inversion), calcite starts to precipitate in *Arctica* shells at 175°C after 4 days.[61] The generally lower inversion temperatures of biogenic aragonite compared to abiogenic aragonite were explained by the degradation of the (inter-crystalline) organic matrix and associated release of water and CO_2 that reduce the reaction temperature

needed for recrystallization.[27,59,62,63] As demonstrated by these experiments, temperature generated during micromilling likely exceeded 175 or 400°C, depending on the availability of water, but remained below 600°C (when decomposition of $CaCO_3$ starts).

Micromilling at higher speed generates more frictional heat and demonstrably not only leads to a larger proportion of calcite, but also a stronger isotope shift.[29] During calcite precipitation, an exchange of oxygen and carbon isotopes with atmospheric water vapor and CO_2 occurs, leading to lower $\delta^{18}O$ and $\delta^{13}C$ values (provided that aragonite was enriched in the heavy isotopes of oxygen and carbon relative to that of H_2O and CO_2 in air) (e.g., Staudigel & Swart[27]; Li et al.[28]). In (fresh) biogenic aragonite, the negative isotope shift is more pronounced because the H_2O and CO_2 released from decaying shell organic matrix during heating is isotopically highly depleted as a consequence of biological fractionation during formation of the shell biopolymers (preference for ^{12}C and ^{16}O).

Although our micromilling experiments were only conducted at a single drill speed (2000 rpm), findings were largely consistent with previous observations. Specifically, the slightly stronger $\delta^{18}O$ and $\delta^{13}C$ shift of micromilled biogenic aragonite compared to abiogenic aragonites (Table 1 and Figure 3A–C) supports the view that exchange with organic matrix-derived oxygen and carbon isotopes occurs during calcite formation. However, the slope of the isotope change (also when combined with the vibromilled data) was steeper than in some previous studies. For example, Waite and Swart[26] likewise reported lower isotope values in micromilled sclerosponges, scleractinian corals, and bivalve shells compared to those manually pounded with an agate mortar and pestle, but they observed a more than sevenfold shallower slope in $\delta^{18}O$ than reported here (0.02‰ vs. 0.15‰ per 1 wt% calcite increase) and $\delta^{13}C$ values showed barely any change (as opposed to 0.1‰ in the present study), except for corals that declined, on average, by ca. 0.05‰ per 1 wt% calcite increase. Waite and Swart[26] interpreted the discrepancies in $\delta^{13}C$ offsets between taxa by differences in skeletal density and ultrastructure, which in turn translate to differences in the organic matrix composition (cf. Milano & Nehrke[64]). Differences in the amount and type of organic matrices could also explain the stronger change in both isotope values of the *Arctica* shell powder(s). If this was a widespread phenomenon and isotope shifts in micromilled shell (or otherwise mechanically prepared shell powder) differed by taxon, existing paleothermometry equations based on machine-ground biogenic aragonite powders (see overview in Grossman[65]) could be intrinsically biased and deviate from thermodynamic predictions. A detailed taxon-specific assessment of isotope effects in pulverized biogenic aragonites would thus be advised in future studies.

4.5 | Mineralogical and isotopic change: effects of water vapor and ACC

In addition to the isotope changes associated with the polymorphic transformation of aragonite, interaction with the shell organic matrix as well as abiogenic aragonite precipitation, other causes should be taken into consideration to explain isotopic and mineralogical patterns of micromilled or vibromilled aragonite powder. As demonstrated by Tobin et al.,[66] isotopes of water (and to a lesser extent CO_2) in air can potentially exchange with the oxygen in aragonite if micromilled powder is heated (70°C) for several hours prior to isotope analysis. Due to larger surface area, finer grained aragonite powder experiences a stronger oxygen isotope shift (up to -0.1‰ per day) than coarser grained material. According to Tobin et al.,[66] CO_2 in air is less important than water as the $\delta^{13}C$ values remained largely unchanged. As an alternative or additional interpretation, we suggest that water absorbed to crystal surfaces cannot be fully removed by these temperatures and will thus contribute to the $\delta^{18}O$ value of the sample. However, our data do not provide unequivocal support for these hypotheses. Although vibromilling with larger balls, higher oscillation frequency, and for longer time should have generated increasingly finer powders that could have attracted larger amounts of water leading to lower $\delta^{18}O$ values, but such a trend was only observed in the shell samples. In addition, cryomilling should have limited the isotopic exchange with water and resulted in lower $\delta^{18}O$ offsets, but this was only observed in the most vigorously ground shell material. Pulverization could have exposed ACC – which was found in all three studied aragonites – to humidity in air, which triggered calcite formation and led to lower isotope values. However, this should also have occurred after manual pounding with an agate mortar and pestle in all three materials, not just in the shell aragonite. Furthermore, increasingly finer grained aragonite powder should have uncovered increasingly larger amounts of ACC, leading to increasingly lower isotope values, which was not observed in the $\delta^{18}O$ values of the aragonite sputnik powders. An adjusted experimental design in future studies may shed light on these hypotheses.

4.6 | Pulverization of aragonite under cooled conditions

In most cases, cryomilling of shell material resulted in larger calcite fractions, but largely invariant isotope values. Additional laser granulometry measurements of the shell material revealed finer particles in the sample milled with the cryomill compared to the sample pounded with an agate mortar and pestle (Data S1). These finer particles may lead to the formation of a larger fraction of agglutinated particles that act as additional milling balls, favoring transformation into calcite. At the same time, the colder reaction environment reduced the decomposition of shell organic materials, which also limited the isotopic exchange rates. Furthermore, agglutinated particles offer lower surface area for potential isotope exchange reactions. It should be noted that grain size distribution curves were only determined for manually pounded shell powder and one cryomilled shell powder. Future studies are therefore needed to determine the grain size distribution curves of all generated powders, for example by laser granulometry, and assess if differences exist depending on the use of liquid nitrogen. Vibromilling in cyclohexane – as done by Momota et al.[41] – could test some of the

above hypotheses as it strongly reduces particle agglutination, serves as a coolant and allows to conduct the pulverization in the absence of air.

4.7 | Recommendations for production of aragonite powder

If possible, samples should be ground by hand with an agate mortar and pestle to obtain the most pristine isotope data. Cryomilling of biogenic aragonite is not recommended because the use of liquid nitrogen typically does not preserve the original isotope signatures better than not using this cooling agent, unless a vigorous grinding technique is applied. More importantly, cryomilling of shell material leads to an increase in calcite content that aggravates the interpretation of isotope data. The isotope bias caused by micromilling can most likely be reduced by much lower drill speeds and lower pressure ("scan speed" in Moon et al.[29]). In our team, micromilling is typically accomplished at 400–800 rpm.

5 | CONCLUSIONS

The milling of biogenic and abiogenic aragonite into powder requires great care to ensure the pristine isotopic signals are preserved and no inversion to calcite occurs. A total of 30 pulverized samples were obtained with 10 different pounding, micromilling, and vibromilling methods that were tested on one biogenic and two abiogenic materials. All powders were reasonably well homogenized (1σ precision errors of 10 measured aliquots: $\delta^{13}C = 0.03‰–0.10‰$, $\delta^{18}O = 0.07‰–0.12‰$). A second ball milling cycle and more energetic vibromilling (larger ball size, higher oscillation frequency, longer grinding duration) resulted in enhanced sample homogeneity, but at the expense of calcite formation and lower isotope values. The results demonstrate that none of the tested pulverization methods, including cryogenic vibromilling, prevented the inversion of aragonite to calcite and decrease of $\delta^{18}O$ and $\delta^{13}C$ values.

The aragonite-to-calcite transformation is multicausal, species-specific, and still not fully understood. It is recommended that the hand-held or computer-controlled micromill be operated at the lowest possible speed and contact pressure kept to a minimum. Manual pounding in an agate mortar and pestle should become the routine method for generating aragonite powders for bulk isotope analyses. If unavoidable, vibromilling should be done with a low oscillation frequency and small milling balls for the shortest possible time (<3 min). Cryogenic vibromilling of shell material should be avoided as it promotes the fractional formation of calcite, which makes the interpretation of the isotope data more complex and challenging. Further research is advised to ascertain the optimal pulverization method (e.g., ideal micromilling speed and contact pressure/scan speed) and evaluate in which cases *in-situ* isotope analytical methods (Secondary Ion Mass Spectrometry) could provide more reliable results.

ACKNOWLEDGMENTS

We thank Ralf Meffert, Tobias Häger, and Michael Maus (JGU Mainz) for laboratory assistance. Financial support from the German Aerospace Center (DLR) and the German Federal Ministry of Education and Research (BMBF) for the project UmWeltWandel under grant no. 01UL2001B is gratefully acknowledged. LJF and DV were funded by the Deutsche Forschungsgemeinschaft (DFG, German Research Foundation) within framework of FOR 2685. BRS has received funding from the European Research Council under the European Union's Horizon 2020 research and innovation program (grant agreement no. 856488).

AUTHOR CONTRIBUTIONS

Katharina E. Schmitt: Conceptualization; investigation; writing—original draft; methodology; visualization; project administration; formal analysis. **Laura Jane Fink:** Investigation. **Anne Jantschke:** Investigation. **Daniel Vigelius:** Investigation. **Bernd R. Schöne:** Funding acquisition; writing—original draft; supervision.

ORCID

Katharina E. Schmitt https://orcid.org/0000-0001-5175-4070

REFERENCES

1. Mook WG. Paleotemperatures and chlorinities from stable carbon and oxygen isotopes in shell carbonate. *Palaeogeography, Palaeoclimatology, Palaeoecology*. 1971;9(4):245-263. doi:10.1016/0031-0182(71)90002-2
2. Wefer G, Berger WH. Isotope paleontology: Growth and composition of extant calcareous species. *Mar Geol*. 1991;100(1–4):207-248. doi:10.1016/0025-3227(91)90234-u
3. Weidman CR, Jones GA, Lohmann K. The long-lived mollusc *Arctica islandica*: A new paleoceanographic tool for the reconstruction of bottom temperatures for the continental shelves of the northern North Atlantic Ocean. *J Geophys Res Oceans*. 1994;99(C9):18305-18314. doi:10.1029/94jc01882
4. Jones DS, Quitmyer IR. Marking time with bivalve shells: Oxygen isotopes and season of annual increment formation. *Palaios*. 1996;11(4):340-346. doi:10.2307/3515244
5. Schöne BR, Castro ADF, Fiebig J, Houk SD, Oschmann W, Kröncke I. Sea surface water temperatures over the period 1884–1983 reconstructed from oxygen isotope ratios of a bivalve mollusk shell (*Arctica islandica*, southern North Sea). *Palaeogeography, Palaeoclimatology, Palaeoecology*. 2004;212(3–4):215-232. doi:10.1016/j.palaeo.2004.05.024
6. Lough JM. Climate records from corals. *Wiley Interdisciplinary Reviews: Climate Change*. 2010;1(3):318-331. doi:10.1002/wcc.39
7. Wang T, Surge D, Walker KJ. Seasonal climate change across the Roman warm period/vandal minimum transition using isotope sclerochronology in archaeological shells and otoliths, Southwest Florida, USA. *Quat Int*. 2013;308:230-241. doi:10.1016/j.quaint.2012.11.013
8. McDermott F. Palaeo-climate reconstruction from stable isotope variations in speleothems: A review. *Quaternary Science Reviews*. 2004;23(7–8):901-918. doi:10.1016/j.quascirev.2003.06.021
9. Dettman DL, Lohmann KC. Microsampling carbonates for stable isotope and minor element analysis: Physical separation of samples on a 20 micrometer scale. *J Sediment Res*. 1995;65(3):566-569. doi:10.1306/d426813f-2b26-11d7-8648000102c1865d
10. Wurster CM, Patterson WP, Cheatham MM. Advances in micromilling techniques: A new apparatus for acquiring high-

resolution oxygen and carbon stable isotope values and major/minor elemental ratios from accretionary carbonate. *Comput Geosci*. 1999; 25(10):1159-1166. doi:10.1016/s0098-3004(99)00052-7

11. Reynolds DJ, Hall IR, Slater SM, Scourse JD, Halloran PR, Sayer MDJ. Reconstructing past seasonal to multicentennial-scale variability in the NE Atlantic Ocean using the long-lived marine bivalve mollusk *Glycymeris glycymeris*. *Paleoceanography*. 2017;32(11):1153-1173. doi:10.1002/2017pa003154
12. Schöne BR, Fiebig J, Pfeiffer M, et al. Climate records from a bivalved methuselah (*Arctica islandica*, Mollusca; Iceland). *Palaeogeography, Palaeoclimatology, Palaeoecology*. 2005;228(1–2):130-148. doi:10.1016/j.palaeo.2005.03.049
13. Peharda M, Puljas S, Chauvaud L, Schöne BR, Ezgeta-Balić D, Thébault J. Growth and longevity of *Lithophaga lithophaga*: What can we learn from shell structure and stable isotope composition? *Mar Biol*. 2015;162(8):1531-1540. doi:10.1007/s00227-015-2690-0
14. Prendergast AL, Stevens RE, Hill EA, Hunt C, O'Connell TC, Barker GW. Carbon isotope signatures from land snail shells: Implications for palaeovegetation reconstruction in the eastern Mediterranean. *Quat Int*. 2017;432:48-57. doi:10.1016/j.quaint.2014.12.053
15. Yanes Y, Al-Qattan NM, Rech JA, Pigati JS, Dodd JP, Nekola JC. Overview of the oxygen isotope systematics of land snails from North America. *Quatern Res*. 2019;91(1):329-344. doi:10.1017/qua.2018.79
16. Colonese AC, Mannino MA, Mayer DBY, et al. Marine mollusc exploitation in Mediterranean prehistory: An overview. *Quat Int*. 2011;239(1–2):86-103. doi:10.1016/j.quaint.2010.09.001
17. Dong J, Eiler J, An Z, et al. Clumped and stable isotopes of land snail shells on the Chinese loess plateau and their climatic implications. *Chem Geol*. 2020;533:119414. doi:10.1016/j.chemgeo.2019.119414
18. Guiguer KRRA, Drimmie R, Power M. Validating methods for measuring $\delta^{18}O$ and $\delta^{13}C$ in otoliths from freshwater fish. *Rapid Commun Mass Spectrom*. 2003;17(5):463-471. doi:10.1002/rcm.935
19. Lojen S, Dolenec T, Vokal B, Cukrov N, Mihelčić G, Papesch W. C and O stable isotope variability in recent freshwater carbonates (river Krka, Croatia). *Sedimentology*. 2004;51(2):361-375. doi:10.1111/j.1365-3091.2004.00630.x
20. Pesenti H, Leoni M, Scardi P. XRD line profile analysis of calcite powders produced by high energy milling. In: *Fifth Size Strain Conference. Diffraction Analysis of the Microstructure of Materials: Garmisch-Partenkirchen, October 7–9, 2007*. Oldenburg Wissenschaftsverlag; 2008:143-150. doi:10.1524/9783486992564-019
21. Burns JH, Bredig MA. Transformation of calcite to aragonite by grinding. *J Chem Phys*. 1956;25(6):1281-1281. doi:10.1063/1.1743198
22. Dandurand JL, Gout R, Schott J. Experiments on phase transformations and chemical reactions of mechanically activated minerals by grinding: Petrogenetic implications. *Tectonophysics*. 1982; 83(3–4):365-386. doi:10.1016/0040-1951(82)90028-2
23. Lin IJ. Implications of fine grinding in mineral processing mechanochemical approach. *Journal of Thermal Analysis and Calorimetry*. 1998;52:453-461. doi:10.1023/a:1010178413725
24. Foster LC, Andersson C, Høie H, Allison N, Finch AA, Johansen T. Effects of micromilling on $\delta^{18}O$ in biogenic aragonite. *Geochemistry Geophysics Geosystems*. 2008;9(4):Q04013. doi:10.1029/2007gc001911
25. Parker JE, Thompson SP, Lennie AR, Potter J, Tang CC. A study of the aragonite-calcite transformation using Raman spectroscopy, synchrotron powder diffraction and scanning electron microscopy. *CrstEngComm*. 2010;12(5):1590-1599. doi:10.1039/b921487a
26. Waite AJ, Swart PK. The inversion of aragonite to calcite during the sampling of skeletal archives: Implications for proxy interpretation. *Rapid Commun Mass Spectrom*. 2015;29(10):955-964. doi:10.1002/rcm.7180
27. Staudigel PT, Swart PK. Isotopic behavior during the aragonite-calcite transition: Implications for sample preparation and proxy interpretation. *Chem Geol*. 2016;442:130-138. doi:10.1016/j.chemgeo.2016.09.013
28. Li C, Shen H, Sheng X, Wei H, Chen J. Kinetics and fractionation of carbon and oxygen isotopes during the solid-phase transformation of biogenic aragonite to calcite: The effect of organic matter. *Palaeogeography, Palaeoclimatology, Palaeoecology*. 2020;556:109876. doi:10.1016/j.palaeo.2020.109876
29. Moon LR, Judd EJ, Thomas J, Ivany LC. Out of the oven and into the fire: Unexpected preservation of the seasonal $\delta^{18}O$ cycle following heating experiments on shell carbonate. *Palaeogeography, Palaeoclimatology, Palaeoecology*. 2021;562:110115. doi:10.1016/j.palaeo.2020.110115
30. Füllenbach CS, Schöne BR, Mertz-Kraus R. Strontium/lithium ratio in aragonitic shells of *Cerastoderma edule* (Bivalvia)—a new potential temperature proxy for brackish environments. *Chem Geol*. 2015;417:341-355. doi:10.1016/j.chemgeo.2015.10.030
31. Doebelin N, Kleeberg R. Profex: A graphical user interface for the Rietveld refinement program BGMN. *J Appl Cryst*. 2015;48(5):1573-1580. doi:10.1107/s1600576715014685
32. León-Reina L, García-Maté M, Álvarez-Pinazo G, et al. Accuracy in Rietveld quantitative phase analysis: A comparative study of strictly monochromatic mo and cu radiations. *J Appl Cryst*. 2016;49(3):722-735. doi:10.1107/s1600576716003873
33. Foster LC, Allison N, Finch AA, Andersson C, Ninnemann US. Controls on $\delta^{18}O$ and $\delta^{13}C$ profiles within the aragonite bivalve *Arctica islandica*. *The Holocene*. 2009;19(4):549-558. doi:10.1177/0959683609104028
34. Thébault J, Schöne BR, Hallmann N, Barth M, Nunn EV. Investigation of Li/ca variations in aragonitic shells of the ocean quahog *Arctica islandica*, Northeast Iceland. *Geochem Geophys Geosyst*. 2009; 10(12). doi:10.1029/2009gc002789
35. Hippler D, Witbaard R, van Aken HM, Buhl D, Immenhauser A. Exploring the calcium isotope signature of *Arctica islandica* as an environmental proxy using laboratory-and field-cultured specimens. *Palaeogeography, Palaeoclimatology, Palaeoecology*. 2013;373:75-87. doi:10.1016/j.palaeo.2011.11.015
36. Wanamaker AD, Gillikin DP. Strontium, magnesium, and barium incorporation in aragonitic shells of juvenile *Arctica islandica*: Insights from temperature controlled experiments. *Chem Geol*. 2019;526:117-129. doi:10.1016/j.chemgeo.2018.02.012
37. Forjanes P, Simonet Roda M, Greiner M, et al. Experimental burial diagenesis of aragonitic biocarbonates: From organic matter loss to abiogenic calcite formation. *Biogeosciences*. 2022;19(16):3791-3823. doi:10.5194/bg-19-3791-2022
38. Holland HA, Schöne BR, Lipowsky C, Esper J. Decadal climate variability of the North Sea during the last millennium reconstructed from bivalve shells (*Arctica islandica*). *The Holocene*. 2014;24(7):771-786. doi:10.1177/0959683614530438
39. Crippa G, Angiolini L, Bottini C, et al. Seasonality fluctuations recorded in fossil bivalves during the early Pleistocene: Implications for climate change. *Palaeogeography, Palaeoclimatology, Palaeoecology*. 2016;446:234-251. doi:10.1016/j.palaeo.2016.01.029
40. Kim ST, Mucci A, Taylor BE. Phosphoric acid fractionation factors for calcite and aragonite between 25 and 75°C: Revisited. *Chem Geol*. 2007;246(3–4):135-146. doi:10.1016/j.chemgeo.2007.08.005
41. Momota H, Senna M, Takagi M. Effects of wet vibro-milling on the polymorphic conversion of aragonite into calcite. *Journal of the Chemical Society, Faraday Transactions 1: Physical Chemistry in Condensed Phases*. 1980;76:790-796. doi:10.1039/f19807600790
42. Lukin S, Tireli M, Stolar T, et al. Isotope labeling reveals fast atomic and molecular exchange in mechanochemical milling reactions. *J am Chem Soc*. 2019;141(3):1212-1216. doi:10.1021/jacs.8b12149.s001

43. Schmidt R, Martin Scholze H, Stolle A. Temperature progression in a mixer ball mill. *International Journal of Industrial Chemistry*. 2016;7(2):181-186. doi:10.1007/s40090-016-0078-8
44. Zhang G, Guo Y, Ao J, Yang J, Lv G, Shih K. Thermally induced phase transformation of pearl powder. *Mater Sci Eng C*. 2013;33(4):2046-2049. doi:10.1016/j.msec.2013.01.016
45. Gillet P, Gérard Y, Willaime C. The calcite-aragonite transition: Mechanism and microstructures induced by the transformation stresses and strain. *Bulletin de Minéralogie*. 1987;110(5):481-496. doi:10.3406/bulmi.1987.7992
46. Pokroy B, Quintana JP, Caspi EAN, Berner A, Zolotoyabko E. Anisotropic lattice distortions in biogenic aragonite. *Nat Mater*. 2004;3(12):900-902. doi:10.1038/nmat1263
47. Pokroy B, Fitch AN, Lee PL, Quintana JP, El'ad NC, Zolotoyabko E. Anisotropic lattice distortions in the mollusk-made aragonite: A widespread phenomenon. *J Struct Biol*. 2006;153(2):145-150. doi:10.1016/j.jsb.2005.10.009
48. Pokroy B, Fitch AN, Zolotoyabko E. Structure of biogenic aragonite ($CaCO_3$). *Cryst Growth des*. 2007;7(9):1580-1583. doi:10.1021/cg060842v
49. Schrader R, Hoffmann B. Über die mechanische Aktivierung von Calciumcarbonat. *Zeitschrift für Anorganische Und Allgemeine Chemie*. 1969;369(1–2):41-47. doi:10.1002/zaac.19693690107
50. Criado JM, Trillo JM. Effects of mechanical grinding on the texture and structure of calcium carbonate. *Journal of the Chemical Society, Faraday Transactions 1: Physical Chemistry in Condensed Phases*. 1975;71:961-966. doi:10.1039/f19757100961
51. Nassif N, Pinna N, Gehrke N, Antonietti M, Jäger C, Cölfen H. Amorphous layer around aragonite platelets in nacre. *Proceedings of the National Academy of Sceinces of the United States of America*. 2005;102(36):12653-12655. doi:10.1073/pnas.0502577102
52. Yoshioka S, Kitano Y. Transformation of aragonite to calcite through heating. *Geochem J*. 1985;19(4):245-249. doi:10.2343/geochemj.19.245
53. Aharon P. Recorders of reef environment histories: Stable isotopes in corals, giant clams, and calcareous algae. *Coral Reefs*. 1991;10(2):71-90. doi:10.1007/bf00571826
54. Gill I, Olson JJ, Hubbard DK. Corals, paleotemperature records, and the aragonite-calcite transformation. *Geology*. 1995;23(4):333-336. doi:10.1130/0091-7613(1995)0232.3.co;2
55. Gillikin DP, De Ridder F, Ulens H, et al. Assessing the reproducibility and reliability of estuarine bivalve shells (*Saxidomus giganteus*) for sea surface temperature reconstruction: Implications for paleoclimate studies. *Palaeogeography, Palaeoclimatology, Palaeoecology*. 2005;228(1–2):70-85. doi:10.1016/j.palaeo.2005.03.047
56. Epstein S, Mayeda T. Variation of O^{18} content of waters from natural sources. *Geochim Cosmochim Acta*. 1953;4(5):213-224. doi:10.1016/0016-7037(53)90051-9
57. Koga N, Nishikawa K. Mutual relationship between solid-state aragonite–calcite transformation and thermal dehydration of included water in coral aragonite. *Cryst Growth des*. 2014;14(2):879-887. doi:10.1021/cg4018689
58. Milano S, Lindauer S, Prendergast AL, et al. Mollusk carbonate thermal behaviour and its implications in understanding prehistoric fire events in shell middens. *J Archaeol Sci Rep*. 2018;20:443-457. doi:10.1016/j.jasrep.2018.05.027
59. Tone T, Koga N. Interplay between thermally induced aragonite–calcite transformation and multistep dehydration in a seawater spiral shell (*Euplica scripta*). *Processes*. 2023;11(6):1650. doi:10.3390/pr11061650
60. Milano S, Prendergast AL, Schöne BR. Effects of cooking on mollusk shell structure and chemistry: Implications for archeology and paleoenvironmental reconstruction. *J Archaeol Sci Rep*. 2016;7:14-26. doi:10.1016/j.jasrep.2016.03.045
61. Casella LA, Griesshaber E, Yin X. Experimental diagenesis: Insights into aragonite to calcite transformation of *Arctica islandica* shells by hydrothermal treatment. *Biogeosciences*. 2017;14(6):1461-1492. doi:10.5194/bg-14-1461-2017
62. Druffel ER, Benavides LM. Input of excess CO_2 to the surface ocean based on $^{13}C/^{12}C$ ratios in a banded Jamaican sclerosponge. *Nature*. 1986;321(6065):58-61. doi:10.1038/321058a0
63. Tone T, Koga N. Thermally induced aragonite–calcite transformation in freshwater pearl: A mutual relation with the thermal dehydration of included water. *ACS Omega*. 2021;6(21):13904-13914. doi:10.1021/acsomega.1c01683
64. Milano S, Nehrke G. Microstructures in relation to temperature-induced aragonite-to-calcite transformation in the marine gastropod *Phorcus turbinatus*. *PLoS ONE*. 2018;13(10):e0204577. doi:10.1371/journal.pone.0204577
65. Grossman EL. Applying oxygen isotope paleothermometry in deep time. *The Paleontological Society Papers*. 2012;18:39-68. doi:10.1017/s1089332600002540
66. Tobin TS, Schauer AJ, Lewarch E. Alteration of micromilled carbonate $\delta^{18}O$ during Kiel device analysis. *Rapid Commun Mass Spectrom*. 2011;25(15):2149-2152. doi:10.1002/rcm.5093

SUPPORTING INFORMATION

Additional supporting information can be found online in the Supporting Information section at the end of this article.

How to cite this article: Schmitt KE, Fink LJ, Jantschke A, Vigelius D, Schöne BR. Isotopic and mineralogic bias introduced by pulverization of aragonite. *Rapid Commun Mass Spectrom*. 2024;38(17):e9842. doi:10.1002/rcm.9842